Electronic Journal of Biotechnology 25 (2017) 64–69

Contents lists available at ScienceDirect

Electronic Journal of Biotechnology

Research article

Effect of miR-125b on dermal papilla cells of goat secondary hair follicle

Guangxian Zhou [a], Chao Yuan [a,b], Xiaolin He [a], Danju Kang [a], Xiaolong Wang [a], Yulin Chen [a,*]

[a] College of Animal Science and Technology, Northwest A&F University, Yangling 712100, China
[b] Lanzhou Institute of Husbandry and Pharmaceutical Sciences of CAAS, Lanzhou 730050, China

ARTICLE INFO

Article history:
Received 10 July 2016
Accepted 17 November 2016
Available online 25 November 2016

Keywords:
Anagen
Antagomir
Cashmere goats
Catagen
Dermal papilla cells
Hair cycle
Hair follicle development
Hair follicle morphogenesis
Luciferase assay
MicroRNAs
Recombinant adenovirus

ABSTRACT

Background: MicroRNAs (miRNAs) are endogenous noncoding RNAs that regulate various biological processes. miR-125b is a miRNA that has been reported to be critical for hair follicle (HF) morphogenesis and development. We identified that the expression of miR-125b varies during an individual hair cycle (anagen, catagen, and telogen) in the skin of cashmere goats. We constructed a gain model (by overexpressing miR-125b) and a loss model (by inhibiting endogenous miR-125b) based on dermal papilla cells (DPCs) to further investigate the role of miR-125b in HF cycle. In addition, we used a dual-luciferase system to highlight the predicated target genes of miR-125b.
Results: We found that miR-125b affects the expression of FGF5, IGF-1, SHH, TNF-α, MSX2, LEF-1, FGF7, NOGGIN, BMP2, BMP4, TGF-β1, and β-catenin. The dual-luciferase assay further validated a direct interaction between miR-125b and FGF5 and TNF-α.
Conclusion: miR-125b affects the expression levels of genes related to hair cycle and may also play a critical role in regulating the periodic development of HF.

1. Introduction

Hair follicles (HFs) consist of more than 20 types of cells, and interactions among these cells induce the formation and cyclic change of HFs [1]. Thus, HFs are dynamic mini-organs that are destined to cycle throughout most of the mammalian life span, with each individual cycle consisting of three phases: anagen (growth), catagen (apoptosis-driven regression), and telogen (rest) [2,3]. This cyclic process is regulated by a series of molecular interactions between epidermal and dermal compartments of a HF. These molecules include signal cytokines, hormones, neurotransmitters, apoptotic factors, and growth factors, and participate in hair cycle by regulating proliferation, differentiation, and apoptosis of different types of cells in the HF [4,5,6,7].

Dermal papilla cells (DPCs) act as a signaling hub and are located in the basal layer of HFs. They are responsible for hair shaft formation, maintenance of HF morphogenesis, regulation of hair growth cycle, and HF regeneration [8,9]. DPCs improve the process of wound healing and induce the formation of hair bud-like structures [10]. Furthermore, these cells are a substitute for HF stem cells in grafted skins [11]. Owing to the pluripotent properties of DPCs [12], cultured DPCs transplanted into the ear of mice can induce neogenesis of HFs under specific conditions [10]. When cultured *in vitro*, DPCs developed a fibroblast-like phenotype with aggregative growth characteristics. However, this feature was gradually lost with increasing number of batches [13].

MicroRNAs (miRNAs) play critical roles in the morphogenesis of HFs and in the hair cycle [12,14,15]. Zhang et al. [16] found that miR-125b is preferentially expressed in progenitor cells of the epidermis and HF. They also observed that miR-125b suppressed HF and skin morphogenesis by repressing the expression of more than 800 predicted conserved miR-125b target transcripts [16]. In cashmere goat skins, the expression of miR-125b in the anagen phase is low, whereas that in both catagen and telogen phases is high [17]. Therefore, we predicted that miR-125b is involved in the morphogenesis of HFs and in the modulation of the HF cycle by altering the expression of key genes. To test this hypothesis, we transfected recombinant miR-125b adenovirus or miR-125b inhibitor into DPCs and validated the transfection using 12 critical genes (FGF5, IGF-1, SHH, TNF-α, MSX2, LEF-1, FGF7, NOGGIN, BMP2, BMP4, TGF-β1, and β-catenin). These two contrasting approaches could reveal whether the expression levels of the 12 genes were related to the hair cycle. Moreover, we performed dual-luciferase assay to further validate the relationship between miR-125b and its predicted target genes.

* Corresponding author.
E-mail address: chenyulin@nwafu.edu.cn (Y. Chen).
Peer review under responsibility of Pontificia Universidad Católica de Valparaíso.

http://dx.doi.org/10.1016/j.ejbt.2016.11.006

2. Materials and methods

2.1. Cell culture

HEK293A and HEK293T cell lines were cultured in DMEM containing 10% fetal bovine serum, 100 U/mL penicillin, and 100 U/mL streptomycin. The DPCs were then isolated, identified, preserved, and cultured according to the protocol described in our previous study [18]. All cells were maintained at 37°C under an atmosphere of 5% CO_2.

2.2. Generation of recombinant adenoviruses

To generate the noncoding adenovirus miRNA-125b (Ad-miR-125b), a 412-bp fragment containing pri-miR-125b was amplified from goat genomic DNA using the primers 5′-ggaAGATCTTCTACTCTAAGTGGAA TC-3′ (forward, BglII is underlined) and 5′-ccgCTCGAGAAATCCAGGAG CTGCCAC-3′ (reverse, XhoI is underlined). The recombinant adenovirus Ad-miR-125b and the negative control (NC) Ad-GFP were propagated in HEK-293A cells according to a previously described protocol [19]. Tissue culture infectious dose 50 method was employed to determine viral titers.

2.3. Identification of miR-125b overexpression

To confirm the overexpression of miR-125b in the DPCs, miR-125b expression was quantified using the stem-loop method with U6 snRNA as the internal control. Ad-miR-125b, Ad-GFP, and PBS were separately added to the DPCs as soon as the cell growth confluence reached approximately 40–50%. All experiments were performed in triplicate, and total miRNAs were harvested 72 h after infection. Multiplicity of infection (MOI) was determined in the DPCs upon successful overexpression.

2.4. Action of Ad-miR-125b and the miR-125b antagomir on DPCs

To investigate the effects of miRNA-125b on DPCs, miR-125b gain- and loss-of-function models were constructed. When cell confluence reached approximately 80%, the Ad-miR-125b or Ad-GFP was added into the medium to a MOI of 300 to infect DPCs. Antagomirs of miR-125b (GenePharama, Shanghai, China) are single-stranded, synthetic, and chemically modified small RNAs that were specifically designed to reduce endogenous miR-125b activity. A double-stranded polynucleotide was used as the NC of miR-125b antagomirs. Antagomirs of miR-125b and corresponding NCs were separately transfected into DPCs at 80% confluence by Lipofectamine 3000 (Invitrogen, USA). The final RNA concentration was 100 nM with an RNA/Lipofectamine 3000 ratio of 2:1. The complex was solved in Opti-MEM reduced serum medium (Invitrogen, USA) according to the manufacturer's protocol. Total RNA was extracted after 72 h of treatment.

2.5. RNA extraction and quantification

Total RNA was prepared in a six-well plate. Cells were rinsed with sterile PBS and RNA was extracted and purified using the Eastep® Super Total RNA Extraction Kit according to the manufacturer's instructions. Approximately, 2000 ng of total RNA was reverse transcribed to synthesize cDNA using the RevertAid First Strand cDNA Synthesis Kit (Thermo, USA) with oligo $dT_{(18)}$ primer and random hexamer primer. Total miRNA was extracted using the miRNA Purification Kit (CWBIO, China). For miR-125b quantification, specific RT primers and U6 RT primers were synthesized by Genscript (Nanjing, China) and reverse transcribed using the RevertAid First Strand cDNA Synthesis Kit (Thermo, USA). Real-time quantitative PCR (qPCR) was performed in triplicate using SYBR Premix Ex Taq II (TaKaRa, Japan) in the BioRad iQ5 system. The $2^{-\Delta\Delta Ct}$ method was used to analyze the relative expression of each gene. qPCR was employed to quantify the expression levels of 12 genes after treatment for 72 h. These genes were strongly related to the HF cycle according to previous studies [2]. All primers are listed in Table 1.

2.6. Dual-luciferase reporter assay

Using the web-based tools RNAhybrid (http://bibiserv.techfak.uni-bielefeld.de/rnahybrid), TargetScan (www.targetscan.org), and miRanda (www.microrna.org), we found that three of the 12 shortlisted genes (FGF5, TGFβ1, and TNF-α) possessed miR-125b target sites. Fragments from these genes containing miR-125b targeted sites were amplified by PCR using primers having *Xho*I and *Not*I sites. Overlap extension PCR was employed to introduce site-directed gene mutagenesis at the miR-125b target sites [20]. The amplified DNA fragments were cloned into the psiCHECKTM-2 Vector (Promega, Madison, WI, USA) at the 3′-end of the Renilla gene by the ligation of the restriction enzyme-digested DNA molecules. The synthetic miR-125b mimics or NC (Genepharma, China) were co-transfected into 293 T cells along with the dual-luciferase vector using Lipofectamine 3000 (Invitrogen, USA). Cells were incubated for 36 h and assayed using a dual-luciferase assay kit (Beyotime, China) according to the manufacturer's instructions. The predicted target genes and all primers used are listed in Table 2.

2.7. Correlation analysis

To explore the extent of the correlation of expression pattern between naturally expressed and simulated genes, we selected the five genes (MSX2, BMP2, TGFB1, FGF7, and FGF5) that were detected in our previous RNA-seq study [21] and in the present study. The quantified expression of these genes and qPCR fold-change values were used for calculation using a general linear model following $\log_{10}$

Table 1
Primers used in the qPCR reaction.

Gene	Primer (5′–3′)	Size (bp)
β-actin	F: CCTCTATGCCAACACAGTGC	211
	R: GTACTCCTGCTTGCTGATCC	
FGF5	F: AGACTGGGCGGGAGTGGTA	106
	R: CTTGGCAGAAAGTGGGTAGAGA	
IGF1	F: TGCCAGTCACATCCTCCTCG	146
	R: ATAAAAGCCCCTGTCTCCAC	
SHH	F: GCTTCGACTGGGTCTACTACG	64
	R: CCCTCACCTGCTTTCACTG	
BMP2	F: CCTTTATACGTGGACTTCAGTG	179
	R: GCCTTGGGAATCTTAGAGTTA	
BMP4	F: CCACCTCCATCAGACACG	173
	R: GTGATGCTTGGGGCTACG	
Noggin	F: CCAGCACTATCTCCACATC	156
	R: ATGAAGCCTGGGTCGTAGT	
TGFβ-1	F: CGTGCTAATGGTGGAATACG	126
	R: CGAGAGAGCAACACAGGTTC	
TNF-α	F: ACGTTGTAGCCAACATCAGC	98
	R: CTGGTTGTCTTTCAGCTCCA	
Msx2	F: GAAACACAAGAGCAATCGGA	148
	R: GACCTGGGTTTCTGTGAGGT	
LEF1	F: GCATCCAGATGGAGGTCTCT	148
	R: CACGGGCACTTTATTTGATG	
FGF7	F: ATGCGCAAATGGATACTGAC	110
	R: GGACTCATGTCATTGCAAGC	
β-catenin	F: CTGCTGTTTTGTTCCGAATGTCT	143
	R: GGGCACCAATATCAAGTCCAA	
RT-primer	TCGTATCCAGTGCAGGGTCCGAGGTATTCGCACTG GATACGACTCACAA	–
miR-125b	F: GCGGCTCCCTGAGACCCTAAC	–
	R: GTGCAGGGTCCGAGGT	
U6	F: CTCGCTTCGGCAGCACA	–
	R: AACGCTTCACGAATTTGCGT	

Table 2
Predicted target sites and primers used for target genes.

Name	Predicted Target Site	Name		Sequence	Product Size
miR-125b	miRNA 3' AGUGUUCAAUCCCAGAGUCCCU- 5'	FGF5-WT	F	ccg**CTCGAG**CAGCAGTAGCACCGCGTCTT	446 bp
	:|: | | ||||||||:		R	attt**GCGGCCGC**ACCACTCCCGCCCAGTCTTT	
FGF5-WT	target 5' AUAUUUGCU-GUGUCUCAGGGGA 3'	FGF5-Mut	FO	TTGGAAATATTTGCTGTAGTCACTTAGATTGTAGGAATACGA	
FGF5-Mut	target 5' ATATTTGCT-GTAGTCACTTAGA 3'		RO	TCGTATTCCTACAATCTAAGTGACTACAGCAAATATTTCCAA	
miR-125b	miRNA 3' AGUGUUCAAUCCCAGAGUCCCU 5'	TGFβ1-WT	F	ccg**CTCGAG**CCGCAAACAGACCCTCC	775 bp
	|||:|||		R	attt**GCGGCCGC**GCCACTGCCGCACAACT	
TGFβ1-WT	target 5' ----------CCUCGGGGC 3'	TGFβ1-Mut	FO	CGCCTCCCCCATGCCGCATCATTATATGCGGCTGCTGCCGCT	
TGFβ1-Mut	target 5' ----------ATCATTATA 3'		RO	AGCGGCAGCAGCCGCATATAATGATGCGGCATGGGGGAGGCG	
miR-125b	miRNA 3' AGUGUUCAAU-CCCAGAGUCCCU 5'	TNF-α-WT	F	ccg**CTCGAG**GCCGCATTGCAGTCTCCTAC	785 bp
	: :| ||| ||| ||||||		R	attt**GCGGCCGC**GACACCTTGACCTCCTGAAT	
TNF-α-WT	target 5' -AGGGAAUUAUGGG-CUCAGGGC 3'	TNF-α-Mut	FO	AGAAAGGGAATTAGGGGTCACATAATGGGCTCCAAGCTTCCA	
TNF-α-Mut	target 5' -AGGGAAUUAUGGG-TCACATAA 3'		RO	TGGAAGCTTGGAGCCCATTATGTGACCCCTAATTCCCTTTCT	

Note: The letters in blue represents key target sites and the letters in red represents the mutant sites and mutated sequences. Lower case letters are primer overhangs to facilitate efficient restriction enzyme binding during digestion. Underlines highlighting the bold letters represent enzyme sites (CTCGAG: *Xho*I; GCGGCCGC: *Not*I).

pretreatment [22]. We speculated that the miR-125b overexpression model (the gain model) mimics the catagen or telogen stages, and the inhibition model (the loss model) mimics the anagen stage from the correlation coefficient.

2.8. Statistical analysis

Student's t-tests (parametric test and unpaired test) were used to determine the significance of the results using SPSS software (version 21.0.0.0, IBM, USA), and GraphPad Prism software (version 6.01, GraphPad Software, Inc., USA) was used to plot the graphs. All data are presented as mean ± SD, and values with $P < 0.05$ were considered statistically significant.

3. Results

3.1. miR-125b expression pattern during hair cycle

To investigate the role of miR-125b in HF regeneration, we initially confirmed miR-125b expression in the skin during the three distinct phases as previously described [17] and subsequently validated the results by qPCR. The expression levels of miR-125b during the three stages are shown in Fig. 1. The expression of miR-125b in the anagen phase was significantly lower than that in the catagen and telogen phases ($P < 0.01$). The expression of miR-125b peaked in the telogen phase (Fig. 1). These results suggest that miR-125b plays a vital role in the hair development cycle and triggers the transition of HFs from the anagen to the catagen and telogen phases.

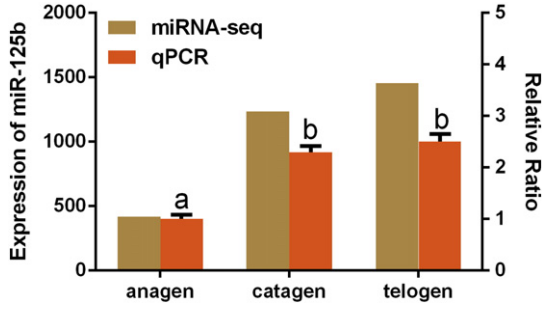

Fig. 1. Relative expression patterns of miR-125b. miR-125b expression during different stages (anagen, catagen, and telogen). The two columns represent miRNA-seq data and qPCR data. Different letters represent statistical significance of differences, "ab" represents $P < 0.01$, and "bb" represents nonsignificant difference.

3.2. Ad-miR-125b and miR-125b antagomir in vitro experiment

The precursor and flanking sequences of miR-125b were amplified, and the miR-125b recombinant adenoviruses (Ad-miR-125b) were successfully recreated (Fig. 2). Compared with cells in the NC group, the expression level of miR-125b was upregulated approximately 2.6-fold in the DPCs infected with Ad-miR-125b ($P < 0.01$) (Fig. 3). Enforced expression of miR-125b (Fig. 4a) led to the significant downregulation of IGF-1 ($P < 0.01$), SHH ($P < 0.01$), TNF-α ($P < 0.01$), MSX2 ($P < 0.01$), LEF-1 ($P < 0.01$), FGF7 ($P < 0.05$), and β-catenin ($P < 0.01$) and significant up-regulation of BMP2 ($P < 0.01$). However, no significant alterations were observed in the expression of BMP4, Noggin, and TGF-β1. The inhibition group was transfected with miR-125b antagomir (Fig. 4b). We found that the expressions of IGF-1 ($P < 0.01$), BMP4 ($P < 0.01$), Noggin ($P < 0.01$), FGF7 ($P < 0.01$), BMP2 ($P < 0.01$), and LEF-1 ($P < 0.05$) were markedly increased, whereas that of SHH ($P < 0.01$) was significantly reduced. No differences were observed in TGF-β1, TNF-α, BDNF, MSX2, and β-catenin expressions between the miR-125b antagomir and control groups.

3.3. Verification of predicted target genes of miR-125b

Dual-luciferase assay was performed to understand the target effect of miR-125b. The relative activity of the gene FGF5 in the treatment group was significantly lower than that in the NC group ($P < 0.01$). A positive reaction for TNF-α gene ($P < 0.05$) was observed in both the wild-type and mutant groups (Fig. 5). Thus, in this study, the treatments showed no significant effects on TGF-β1. Therefore, we conclude that this site may not be a target site of miR-125b.

3.4. Gene expression correlation pattern analysis

To understand the physiological state of the DPCs following treatments with the two contrasting approaches, we performed correlation analysis for the data obtained for the five genes: MSX2, BMP2, TGFB1, FGF7, and FGF5. We found that the expression patterns of these genes is similar to that of goat skins during the three phases, and the correlation coefficients were higher than 0.91. The expression patterns of the five genes in the gain model were consistent with the anagen phase (Fig. 6a). The patterns were much closer to the telogen

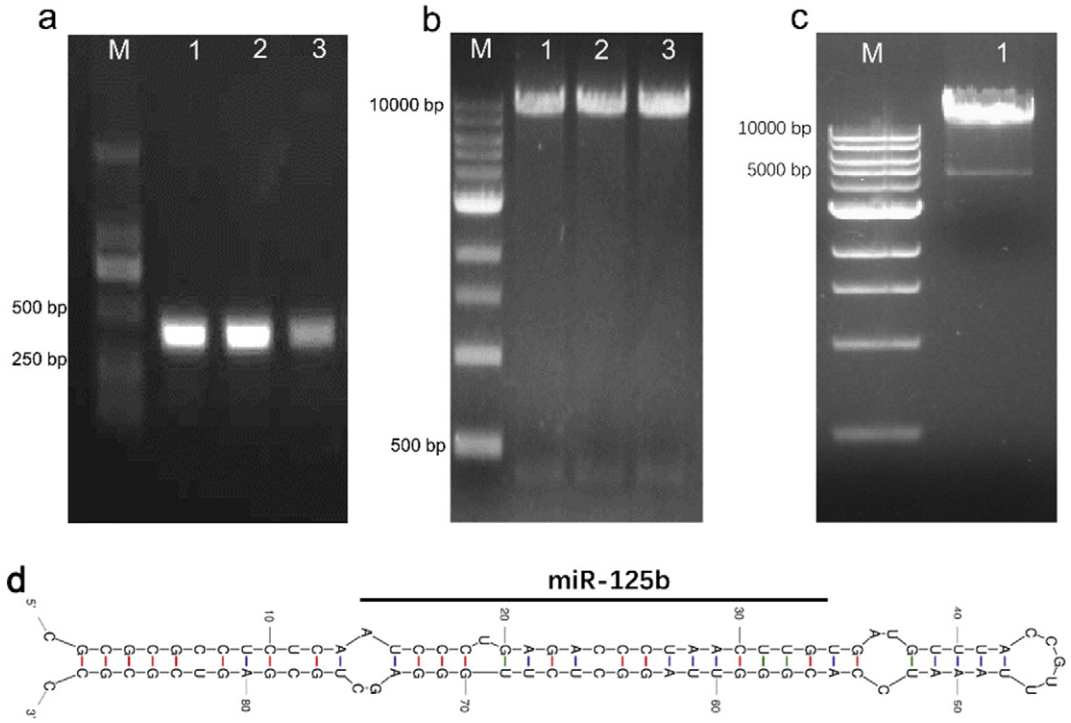

Fig. 2. miR-125b adenovirus construction. (a) Precursor and flanking PCR products of miR-125b (lanes 1–3, amplification product 412 bp). (b) pAdTrack-cmv-miR-125b were digested by BglII and XhoI (lanes 1–3, enzyme-digested products 9220 and 412 bp). (c) Ad-miR-125b were digested by PacI (lane 1, enzyme-digested products 30 and 4.5 kb). (d) MFOLD-predicted structure of miR-125b and mature miRNA. M refers to DNA maker; lanes 1, 2, and 3 within the same gel represent three replicates.

than that to the catagen in the loss model (Fig. 6b). These results indicated that the overexpression of miR-125b could induce the transition of DPCs from the anagen to the catagen and telogen phases.

4. Discussion

To explore the role of miR-125b in DPCs, we overexpressed miR-125b adenovirus and miR-125b antagomirs in mid-anagen secondary DPCs and tested the expression of 12 genes associated with hair growth cycle. Dual-luciferase assay showed that among the predicted genes, FGF5 and TNF-α could be directly regulated by miR-125b.

Our findings revealed that the expression of miR-125b was high in the telogen phase and low in the anagen phase, suggesting a regulatory role of miR-125b during periodic growth. miR-125b showed abundant expression in the stem cells of HF, which decreased after differentiation [18]. Upregulation of miR-125b in transgenic mice resulted in the thickening of the skin, extension of sebaceous glands, and failure to form a coat by inhibiting the differentiation of HF stem cells [16]. DPCs play important roles in HF period transitions [23,24]. Therefore, cultured DPCs are a feasible model to study periodically alternating HFs. Moreover, changes in the expression of genes in DPCs can be considered alternative markers. The 12 selected genes in our study (FGF5, IGF-1, SHH, TNF-α, MSX2, LEF-1, FGF7, NOGGIN, BMP2, BMP4, TGF-β1, and β-catenin) were proven to be associated with both HF morphogenesis and cycling [2].

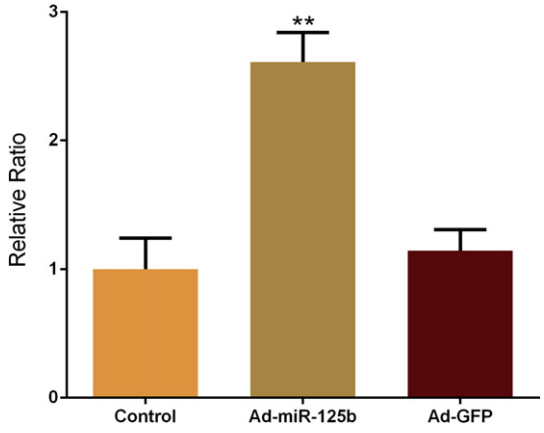

Fig. 3. Relative expression of miR-125b. PBS was added to the control group, and U6 snRNA was used as an internal control for quantification. The fold increases are calculated relative to the control group. Data are given as mean ± SD from three independent experiments (**$P < 0.01$).

FGF5, IGF-1, FGF7, and TGF-β1 are growth factors; however, the functional mechanism of these factors on HF cycle remains unclear. FGF5 is regarded as a crucial regulator of hair length in humans, and blocking FGF5 in the human scalp selectively enhanced the growth of eyelashes [25]. IGF-1 is an important factor that promotes mitosis during HF development and stimulates the formation of epidermal cells and the proliferation and differentiation of DPCs [26]. TGF-β1 induces the transition of HFs into the regression phase, and its overexpression extends the duration of the catagen phase [27,28]. In our study, overexpression of miR-125b promoted the downregulation of FGF5, IGF-1, FGF7, and TGF-β1, whereas inhibition of miR-125b led to opposite results. Although miR-125b may affect these genes indirectly, the synergy of these genes prompted their expression during the HF cycle.

Published reports revealed reciprocal requirements for MSX2/BMP/Wnt/TNF-α, Wnt/β-catenin, and SHH/NOGGIN/LEF1 signaling pathways in the induction of HF growth [29,30]. BMP signaling controlled HF morphogenesis and cyclic changes through the regulation of proliferation and differentiation of the hair matrix; BMP2 was highly expressed during the resting phase and was suppressed during the anagen phase. Thus, the expression of BMP2 maintained the HFs in a resting state [31,32]. The interaction between BMP4 and BMPR-1A influenced secondary follicle cell proliferation; noggin is an antagonist of BMP4 that suppresses BMP4 expression during the telogen phase and increasing SHH expression in epithelial cells, and noggin-SHH

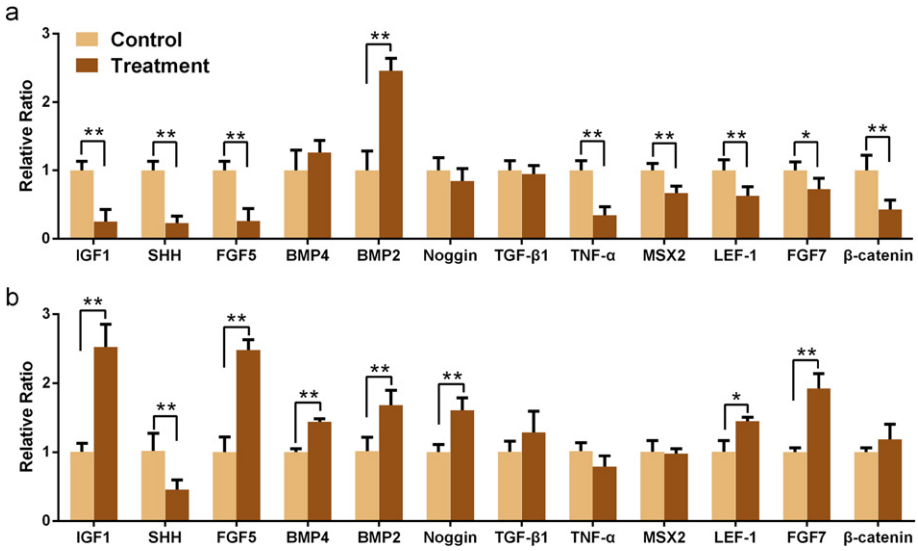

Fig. 4. Expression of 12 genes in different treatment groups. Red bars represent the control group, whereas blue bars represent the treatment group. (a) Ad-miR-125b treatment leads to the overexpression of miR-125b; (b) miR-125b antagomir treatment inhibits endogenous miR-125b ($0.01 < {}^{*}P < 0.05$; ${}^{**}P < 0.01$).

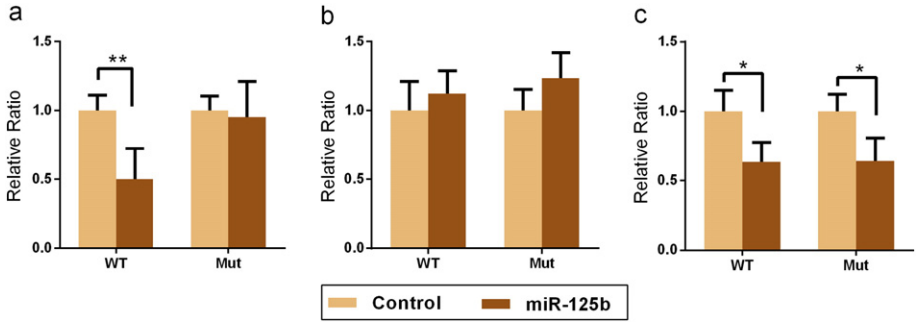

Fig. 5. Dual-luciferase array. Red bars depict control with nontargeting dsDNA treatment, and blue bars depict results after treatment with miR-125b mimics. ${}^{*}P < 0.05$, ${}^{**}P < 0.01$.

pathway signaling could promote HF transition from the telogen to the anagen phase [30,33]. Noggin has been reported to regulate DP development through the induction of proliferation of HF cells interacting with LEF-1 [34]. MSX2 is a member of the homeobox gene family, and knockout mice showed a series of abnormal phenomena, *e.g.*, progressive loss of hair, shortened HF growth cycles, and prolonged regression and resting stages. A previous study revealed the cooperation between MSX2, BMP, and Foxn1 that results in the synthesis of hair keratin [35]. TNF-α transgenic mice showed increased birth weight, slow additional hair growth, and occurrence of skin necrosis following the addition of a cuticle on the skin at 3–4 weeks [36]. β-catenin, an important factor of the Wnt signaling pathway, can accelerate hair growth after activation, whereas loss of β-catenin can block the HF morphogenesis. The expression of β-catenin was noticeably different between the three phases, with high expression in the anagen phase and low expression during both the catagen and telogen phases. The results revealed that β-catenin plays an important role in HF and the hair growth cycle [37,38].

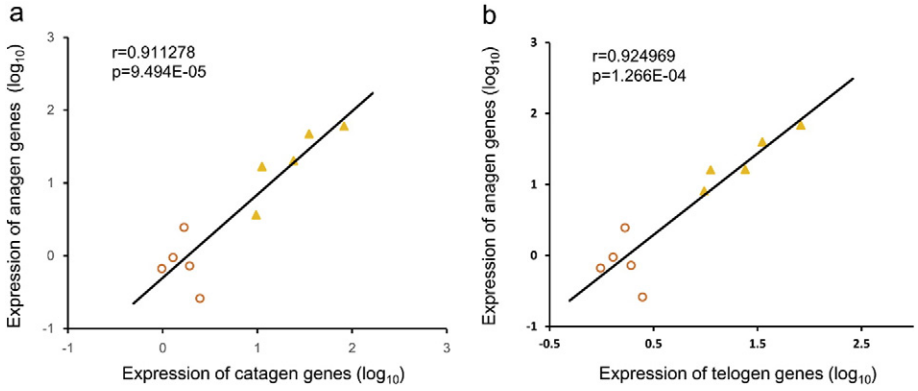

Fig. 6. Correlation analysis of gene expression. Correlation between genes expressed in the anagen with the catagen (a) or telogen (b), as measured by qPCR and RNA-seq. The triangle markers represent RNA-seq data, and the circle markers represent qPCR data.

The dual-luciferase assay revealed the direct regulation of FGF5 and TNF-α by miR-125b. We thus speculate that miR-125b could modulate the HF cycle by targeting FGF5 and TNF-α. The correlation of the two models was similar to that of the anagen and telogen phases during conventional farming; therefore, we could simulate the growth of HFs through the regulation of miR-125b expression. Interestingly, FGF5 and TNF-α could induce anagen–catagen transition during the hair cycle [39,40], whereas miR-125b could reduce the expression of the two. HF cycle is a complex process, and a single stripping phenomenon cannot explain the end results. Several intriguing aspects in the hair cycle remain to be identified.

5. Conclusion

In the present study, we have provided novel insights into the mechanism of the HF growth cycle, with miR-125b participating in the modulation of hair growth by targeting FGF5 and TNF-α. miR-125b expression was relatively low during the anagen phase and regulates hair growth. When the growth of the HFs transitioned into catagen and telogen phases, miR-125b expression was found to be upregulated. We identified the amount of miR-125b required to modulate gene expression in DPCs and trigger the transition of DPCs into different growth phases *in vitro*. We found that FGF5 and TNF-α can be regulated by miR-125b and thus affect HFs. These findings significantly extend our understanding of the regulatory function of miR-125b in HF regeneration.

Financial support

This work was supported by National Natural Science Foundation of China (No. 31372279) and International Cooperation Project of Shaanxi Province (2014KW14-01).

Conflict of interest

The authors declare that they have no competing interests.

References

[1] Paus R, Cotsarelis G. The biology of hair follicles. N Engl J Med 1999;341:491–7. http://dx.doi.org/10.1056/NEJM199908123410706.
[2] Stenn K, Paus R. Controls of hair follicle cycling. Physiol Rev 2001;81:449–94.
[3] Schneider MR, Schmidt-Ullrich R, Paus R. The hair follicle as a dynamic miniorgan. Curr Biol 2009;19:132–42. http://dx.doi.org/10.1016/j.cub.2008.12.005.
[4] Lin B, Wang J, Miao Y, Liu Y, Jiang W, Fan ZX, et al. Cytokine loaded layer-by-layer ultrathin matrices to deliver single dermal papilla cells for spot-by-spot hair follicle regeneration. J Mater Chem B 2016;4:489–504. http://dx.doi.org/http://dx.doi.org/10.1039/C5TB02265G.
[5] Inui S, Itami S. Androgen actions on the human hair follicle: Perspectives. Exp Dermatol 2013;22:168–71. http://dx.doi.org/10.1111/exd.12024.
[6] Wang X, His TC, Guerrero-Juarez CF, Pham K, Cho K, McCusker CD, et al. Principles and mechanisms of regeneration in the mouse model for wound-induced hair follicle neogenesis. Regeneration 2015;2:169–81. http://dx.doi.org/10.1002/reg2.38.
[7] Krause K, Foitzik K. Biology of the hair follicle: The basics. Semin Cutan Med Surg 2006;25:2–10. http://dx.doi.org/10.1016/j.sder.2006.01.002.
[8] Thangapazham RL, Klover P, Wang JA, Zheng Y, Devine A, Li S, et al. Dissociated human dermal papilla cells induce hair follicle neogenesis in grafted dermal-epidermal composites. J Invest Dermatol 2014;134:538–40. http://dx.doi.org/10.1038/jid.2013.337.
[9] Higgins CA, Chen JC, Cerise JE, Jahoda CA, Christiano AM. Microenvironmental reprogramming by three-dimensional culture enables dermal papilla cells to induce de novo human hair-follicle growth. Proc Natl Acad Sci U S A 2013;110:19679–88. http://dx.doi.org/10.1073/pnas.1309970110.
[10] Jahoda CA, Reynolds AJ, Oliver RF. Induction of hair growth in ear wounds by cultured dermal papilla cells. J Invest Dermatol 1993;101:584–90. http://dx.doi.org/http://dx.doi.org/10.1111/1523-1747.ep12366039.
[11] Leiros GJ, Kusinsky AG, Drago H, Bossi S, Sturla F, Castellanos ML, et al. Dermal papilla cells improve the wound healing process and generate hair bud-like structures in grafted skin substitutes using hair follicle stem cells. Stem Cells Transl Med 2014;3:1209–19. http://dx.doi.org/10.5966/sctm.2013-0217.
[12] Andl T, Murchison EP, Liu F, Zhang Y, Yunta-Gonzalez M, Tobias JW, et al. The miRNA-processing enzyme dicer is essential for the morphogenesis and maintenance of hair follicles. Curr Biol 2006;16:1041–9. http://dx.doi.org/10.1016/j.cub.2006.04.005.
[13] Jahoda CA, Oliver RF. Vibrissa dermal papilla cell aggregative behaviour *in vivo* and *in vitro*. J Embryol Exp Morphol 1984;79:211–24.
[14] Mardaryev AN, Ahmed MI, Vlahov NV, Fessing MY, Gill JH, Sharov AA, et al. Micro-RNA-31 controls hair cycle-associated changes in gene expression programs of the skin and hair follicle. FASEB J 2010;24:3869–81. http://dx.doi.org/10.1096/fj.10-160663.
[15] Andl T, Botchkareva NV. MicroRNAs (miRNAs) in the control of HF development and cycling: The next frontiers in hair research. Exp Dermatol 2015;24:821–6. http://dx.doi.org/http://dx.doi.org/10.1111/exd.12785.
[16] Zhang L, Stokes N, Polak L, Fluchs E. Specific microRNAs are preferentially expressed by skin stem cells to balance self-renewal and early lineage commitment. Cell Stem Cell 2011;8:294–308. http://dx.doi.org/10.1016/j.stem.2011.01.014.
[17] Yuan C, Wang X, Geng R, He X, Qu L, Chen Y. Discovery of cashmere goat (*Capra hircus*) microRNAs in skin and hair follicles by Solexa sequencing. BMC Genomics 2013;14:511. http://dx.doi.org/10.1186/1471-2164-14-511.
[18] He X, Chao Y, Zhou G, Chen Y. Fibroblast growth factor 5-short (FGF5s) inhibits the activity of FGF5 in primary and secondary hair follicle dermal papilla cells of cashmere goats. Gene 2016;575:393–8. http://dx.doi.org/10.1016/j.gene.2015.09.034.
[19] Luo J, Deng ZL, Luo X, Tang N, Song WX, Chen J, et al. A protocol for rapid generation of recombinant adenoviruses using the AdEasy system. Nat Protoc 2007;2:1236–47. http://dx.doi.org/10.1038/nprot.2007.135.
[20] Liu H, Naismith JH. An efficient one-step site-directed deletion, insertion, single and multiple-site plasmid mutagenesis protocol. BMC Biotechnol 2008;8:91. http://dx.doi.org/http://dx.doi.org/10.1186/1472-6750-8-91.
[21] Geng R, Yuan C, Chen Y. Exploring differentially expressed genes by RNA-seq in cashmere goat (*Capra hircus*) skin during hair follicle development and cycling. PLoS One 2013;8: e62704. http://dx.doi.org/10.1371/journal.pone.0062704.
[22] Wang T, Jiang A, Guo Y, Tan Y, Tang G, Mai M, et al. Deep sequencing of the transcriptome reveals inflammatory features of porcine visceral adipose tissue. Int J Biol Sci 2013;9:550–6. http://dx.doi.org/10.7150/ijbs.6257.
[23] Rahmani W, Abbasi S, Hagner A, Raharjo E, Kumar R, Hotta A, et al. Hair follicle dermal stem cells regenerate the dermal sheath, repopulate the dermal papilla, and modulate hair type. Dev Cell 2014;31:543–58. http://dx.doi.org/10.1016/j.devcel.2014.10.022.
[24] Chi W, Wu E, Morgan BA. Dermal papilla cell number specifies hair size, shape and cycling and its reduction causes follicular decline. Development 2013;140:1676–83. http://dx.doi.org/10.1242/dev.090662.
[25] Higgins CA, Petukhova L, Harel S, Ho YY, Drill E, Shapiro L, et al. FGF5 is a crucial regulator of hair length in humans. Proc Natl Acad Sci U S A 2014;111:10648–53. http://dx.doi.org/10.1073/pnas.1402862111.
[26] Li J, Yang Z, Li Z, Gu L, Wang Y, Sung C. Exogenous IGF-1 promotes hair growth by stimulating cell proliferation and down regulating TGF-β1 in C57BL/6 mice *in vivo*. Growth Horm IGF Res 2014;24:89–94. http://dx.doi.org/10.1016/j.ghir.2014.03.004.
[27] Soma T, Ogo M, Suzuki J, Takahashi T, Hibino T. Analysis of apoptotic cell death in human hair follicles *in vivo* and *in vitro*. J Invest Dermatol 1998;111:948–54.
[28] Foitzik K, Lindner G, Mueller-Roever S, Maurer M, Botchkareva N, Botchkarev V, et al. Control of murine hair follicle regression (catagen) by TGF-β1 *in vivo*. FASEB J 2000; 14:752–60.
[29] Zhang Y, Tomann P, Andl T, Gallan NM, Huelsken J, Jerchow B, et al. Reciprocal requirements for EDA/EDAR/NF-kB and Wnt/β-catenin signaling pathways in hair follicle induction. Dev Cell 2009;17:49–61. http://dx.doi.org/http://dx.doi.org/10.1016/j.devcel.2009.05.011.
[30] Woo WM, Zhen HH, Oro AE. Shh maintains dermal papilla identity and hair morphogenesis via a Noggin-Shh regulatory loop. Genes Dev 2012;26:1235–46. http://dx.doi.org/10.1101/gad.187401.112.
[31] Rendl M, Polak L, Fuchs E. BMP signaling in dermal papilla cells is required for their hair follicle-inductive properties. Genes Dev 2008;22:543–57. http://dx.doi.org/http://dx.doi.org/10.1101/gad.1614408.
[32] Plikus MV, Mayer JA, de la Cruz D, Baker RE, Maini PK, Maxson R, et al. Cyclic dermal BMP signalling regulates stem cell activation during hair regeneration. Nature 2008; 451:340–4. http://dx.doi.org/10.1038/nature06457.
[33] Botchkarev VA, Botchkareva NV, Sharov AA, Gilchrest BA, Funa K, Huber O. Modulation of BMP signaling by noggin is required for induction of the secondary (Nontylotrich) hair follicles. J Invest Dermatol 2002;118:3–10. http://dx.doi.org/http://dx.doi.org/10.1046/j.1523-1747.2002.01645.x.
[34] Kobielak K, Stokes N, de la Cruz J, Polak L, Fuchs E. Loss of a quiescent niche but not follicle stem cells in the absence of bone morphogenetic protein signaling. Proc Natl Acad Sci U S A 2007;104:10063–8. http://dx.doi.org/10.1073/pnas.0703004104.
[35] Ma L, Liu J, Wu T, Plikus M, Jiang TX, Bi Q, et al. 'Cyclic alopecia' in *Msx2* mutants: Defects in hair cycling and hair shaft differentiation. Development 2003;130: 379–89. http://dx.doi.org/10.1242/dev.00201.
[36] Ruckert R, Lindner G, Bulfone-Paus S, Paus R. High-dose proinflammatory cytokines induce apoptosis of hair bulb keratinocytes *in vivo*. Br J Dermatol 2000;143:1036–9. http://dx.doi.org/10.1046/j.1365-2133.2000.03784.x.
[37] Enshell-Seijffers D, Lindon C, Kashiwagi M, Morgan BA. β-catenin activity in the dermal papilla regulates morphogenesis and regeneration of hair. Dev Cell 2010; 18:633–42. http://dx.doi.org/10.1016/j.devcel.2010.01.016.
[38] Schmidt-Ullrich R, Paus R. Molecular principles of hair follicle induction and morphogenesis. Bioessays 2005;27:247–61. http://dx.doi.org/10.1002/bies.20184.
[39] Hebert JM, Rosenquist T, Gotz J, Martin GR. Fgf5 as a regulator of the hair-growth cycle: Evidence from targeted and spontaneous mutations. Cell 1994;78:1017–25. http://dx.doi.org/10.1016/0092-8674(94)90276-3.
[40] Hoffmann R, Eicheler W, Huth A, Wenzel E, Happle R. Cytokines and growth factors influence hair growth *in vitro*. Possible implications for the pathogenesis and treatment of alopecia areata. Arch Dermatol Res 1996;288:153–6. http://dx.doi.org/http://dx.doi.org/10.1007/BF02505825.